

The preparation and characterization of ultrafine cobalt-iron oxides

A. C. C. TSEUNG, J. R. GOLDSTEIN

Department of Chemistry, The City University, London, UK

Seven ultrafine samples (125 to 60 m²/g) of the cobalt-iron oxide series, Co_xFe_{3-x}O₄, with 0 ≤ x ≤ 3, were prepared by co-precipitation of the metal hydroxides, followed by dehydration of the hydroxide at 100°C. X-ray and chemical analyses confirmed that true spinels were formed. The electrical conductivity and the activation energy for conduction of the powders were determined, and used to define the electronic structure of this series in conjunction with theoretical considerations based on crystal field theory.

1. Introduction

The cobalt-iron oxide series can be represented by the general formula Co_xFe_{3-x}O₄, with 0 ≤ x ≤ 3. This series, which has a spinel structure, is of considerable interest since it is strongly magnetic [1] and is active towards the oxidation of CO and NO [2] as well as H₂O₂ decomposition [3]. The simplest type of spinel oxide possesses the general formula AB₂O₄ where A and B are divalent and trivalent metal ions respectively [4]. The unit cell consists of thirty-two cubic close packed oxide ions. The face-centred cubic spinel structure can be "fully normal" or "fully inverse". In the former case, each A^{II} ion is tetrahedrally co-ordinated by four and each B^{III} ion octahedrally co-ordinated by six oxide neighbours; furthermore, each oxide ion is bound to one A^{II} and to three B^{III} ions in octahedral sites. The situation is reversed in "fully inverse" spinels, with one half of the B^{III} occupying the tetrahedral sites, while the rest of these ions, together with all the A^{II} ions, are distributed at random over the octahedral sites. However, only four structures have been established in the literature for the cobalt-iron oxide series [5-7].

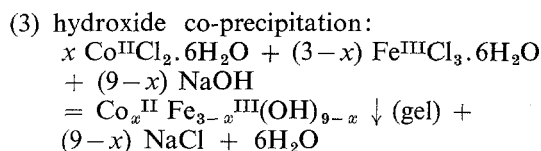
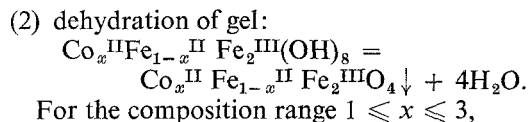
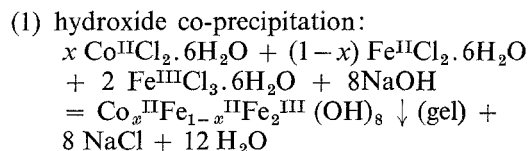
x = 0, [Fe^{III}]_t [Fe^{II} Fe^{III}]_o O₄²⁻ fully inverse
 x = 1, [Fe^{III}]_t [Co^{II} Fe^{III}]_o O₄²⁻ fully inverse
 x = 2, [Co^{II}]_t [Co^{III} Fe^{III}]_o O₄²⁻ fully normal
 x = 3, [Co^{II}]_t [Co^{III} Co^{III}]_o O₄²⁻ fully normal
 where the subscripts t and o stand for tetrahedral and octahedral sites respectively. Since the magnetic and catalytic properties are significantly enhanced by increased surface area, it is of interest to prepare ultrafine cobalt-iron oxide

spinels over a wide range of x values and to determine their structure, especially the distribution of cations at the different crystallographic sites, since this is responsible for their physical and chemical behaviour.

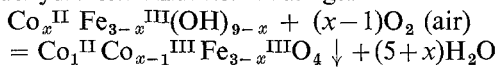
2. Experimental

2.1. Preparation of ultrafine cobalt-iron oxides

Of all the potential methods [8, 9] the hydroxide co-precipitation technique seemed to offer the best chance of success in achieving the highest surface area, since the temperature required is only 100°C [10]. Analar grade cobalt chloride, ferric chloride, sodium hydroxide and Laboratory grade ferrous chloride (99%) (Hopkin and Williams Ltd) were used in this study. For the composition range 0 ≤ x ≤ 1, the reaction equation is given by:



(4) dehydration oxidation of the gel



100 ml solutions containing 0.15M of metal ions, were prepared by dissolving the appropriate amounts of metal chlorides according to (1) or (3) in distilled, de-aerated water. The mixed metal salt solution was then rapidly added with continual stirring to 50 ml of de-aerated, freshly prepared 6N NaOH solution at room temperature. The pH of the reaction mixture was measured by a Vibret pH meter (E.I.L. Ltd). The pH ranged from 8 for $x = 0$ to about 11 for $x = 3$ and was then adjusted to a value of 12.5 [10] by further addition of 6N NaOH from a burette. At this stage, the reaction mixture, which was in the form of a dark gel, was dehydrated on a steam bath for an hour. On reaching 95°C, the reaction mixture became clear and a black powder – the spinel phase, precipitated. This precipitate was filtered and washed repeatedly with distilled water until it was free of alkali. It was then dried overnight at 100°C and the resultant powder was crushed in an agate mortar. Seven samples were prepared, with x values of 0, 0.6, 1.0, 1.5, 2.0, 2.4 and 3.0.

2.2. Chemical analysis of cobalt-iron oxides

The cobalt-iron oxides were analysed for total Co and Fe content gravimetrically by using the zinc oxide separation method [11], whilst the concentration of Co^{III} and Fe^{II} were analysed according to the method devised by Smiltens [12]. The method assumes that if a cobalt-iron oxide containing Fe^{II} is dissolved in a non-oxidizing acidic medium, all the Fe will pass into solution. This can then be quantitatively analysed by using standard KMnO_4 solution. If the sample is expected to contain Co^{III} , a known excess of ferrous ammonium sulphate is added to the acid before dissolving the oxide. As Co^{III} enters the solution, it oxidizes some of the introduced Fe^{II} to Fe^{III} , and this quantity, corresponding to the original amount of Co^{III} , is ascertainable by titrating with standard KMnO_4 solution.

2.3. Surface area measurement and X-ray powder diffraction studies

The surface area of the samples were measured by the BET technique using nitrogen as the adsorbate at -196°C . X-ray powder photographs were taken of all the samples, using a

Philips X-ray machine with a molybdenum target.

2.4. Electrical conductivity measurement

A Wayne-Kerr ac Conductivity Bridge (1592 Hz) was used to measure the conductivity of the samples whilst they were under compression in a steel die which had a thick teflon lining. The pressure was applied with a "G" Clamp. The powders were pressed to 75% of the theoretical density before measurements were taken. For measurement at higher temperatures, the die and the clamp were encased with a thick polythene bag and immersed in a thermostatically regulated oil bath.

3. Results and discussion

3.1. Chemical composition of cobalt-iron oxides

As shown in Table I, all seven samples of cobalt-iron oxides in the $\text{Co}_x\text{Fe}_{3-x}\text{O}_4$ series were successfully prepared, though there were slight deviations from the intended composition in some of the samples.

It is of interest to note that in four of the above cases, some free Fe_2O_3 or Co_3O_4 is present. Let us consider the species most likely to be formed during the co-precipitation and gel dehydration-oxidation reactions in separate cobalt and iron systems.

In aqueous solution, free from complexing agents such as amines, the only stable state for cobalt is as Co^{II} . When NaOH solution is added to a solution containing Co^{II} at room temperature, $\text{Co}(\text{OH})_2$ is precipitated. The solid hydroxide is susceptible to slow air oxidation at room temperature, forming initially a hydrated oxide $\text{Co}_2\text{O}_3 \cdot \text{H}_2\text{O}$ [13]. The oxidation continues, especially at higher temperatures (100°C), to give Co_3O_4 .

In the case of iron, both divalent and trivalent states are stable in aqueous solution. When sodium hydroxide is added to a solution containing Fe^{II} , a white precipitate of $\text{Fe}(\text{OH})_2$ is formed. This is susceptible to air oxidation, and darkens in colour, forming ferric hydroxide (red brown), or, in the presence of excess alkali, the black oxide, Fe_3O_4 . When NaOH solution is added to a solution containing Fe^{III} , the hydrated oxide $\alpha\text{-Fe}_2\text{O}_3 \cdot \text{H}_2\text{O}$ is formed, which soon aggregates to a colloidal ferric hydroxide gel [15].

The above survey shows that the main products of dehydration-oxidation reactions in cobalt and iron hydroxide gels are Co_3O_4 ,

Fe_3O_4 and $\alpha\text{-Fe}_2\text{O}_3$. All of these products possess the spinel structure. Consequently if a solid solution of cobalt and iron hydroxides was subjected to dehydration-oxidation, the product should also possess a spinel structure and in fact should be a cobalt-iron oxide of composition determined by the cobalt/iron ratio, provided the cobalt and iron cations can be precipitated simultaneously. The hydroxides should form a true solid solution, since the ionic radii of the metal cations are similar – $\text{Co}^{\text{II}} = 0.82 \text{ \AA}$, $\text{Fe}^{\text{II}} = 0.83 \text{ \AA}$ [1].

For the simultaneous precipitation of the hydroxides, a high initial pH is required. The solubility product for $\text{Co}(\text{OH})_2$ at 25°C [16] is 6.3×10^{-16} , and a pH of at least 10 is needed for the complete co-precipitation of Co^{II} [17]. $\text{Fe}(\text{OH})_3$ has a very low solubility product (2.0×10^{-39} at 25°C [17]) and Fe^{III} begins to precipitate even in slightly acidic solutions of pH 4. Hence the initial pH of the reaction mixture (always adjusted to 12.5) [10] should suffice at least for the symmetrical ferrite.

For the unsymmetrical ferrites with $0 < x < 1$, the reactant solution contains increasing amount of Fe^{II} substituted for Co^{II} . However, the solubility product of $\text{Fe}(\text{OH})_2$ (8.0×10^{-16} at 25°C) [16], is close to that of $\text{Co}(\text{OH})_2$, so full precipitation should still result if the pH is above 10.

Identical considerations apply to cobalt-iron oxides with $1 < x < 3$. A high initial pH is especially vital for complete hydroxide precipitation, since Co^{II} , with a relatively high solubility product as $\text{Co}(\text{OH})_2$, increasingly replaces Fe^{III} with a much lower one as $\text{Fe}(\text{OH})_3$, in the reaction mixture. The high pH (12.5) used, however, is adequate for complete precipitation. Thus, over the complete composition range $0 \leq x \leq 3$, fully precipitated hydroxides will be formed.

The dehydration-oxidation to the final spinel phase should produce spinel lattices with the correct metal ion distribution. Equation 1 gives the reactions involved for the spinel formation when $0 \leq x \leq 1$ and accordingly contains excess Fe^{II} over the symmetrical ferrite. This is based on the assumption that the spinel phase is formed rapidly and that air oxidation of Fe^{II} or Co^{II} in the reaction mixture proceeds relatively slowly. Both Sato [10] and Elmore [18] reported a low loss of Fe^{II} (maximum 5%) by air oxidation of hydroxide in $\text{Co}_1\text{Fe}_2\text{O}_4$ and $\text{Fe}_1\text{Fe}_2\text{O}_4$ preparations. Fe^{II} loss was reduced in the present

study by using de-aerated solutions.

In order to introduce Co^{III} into the lattice in compositions with $1 < x \leq 3$, the dehydration reaction must be accompanied by air oxidation of Co^{II} (Equation 4). This is in agreement with the work of Besson [14], who showed that when aqueous suspensions of $\text{Co}(\text{OH})_2$ are boiled in air, Co_3O_4 is the main product.

3.2. BET surface area of cobalt-iron oxides

Fig. 1 shows the variation of BET surface area with x , indicating that it decreases with increasing cobalt content. The decrease is very much more rapid between $0 < x < 1$. Despite the significant decrease in surface area, the surface areas of all the cobalt-iron oxides are very high (125 to 60 m^2/g). $\text{Co}_0\text{Fe}_3\text{O}_4$ has the highest surface area, whilst $\text{Co}_3\text{Fe}_0\text{O}_4$ has the lowest surface area. When metal hydroxides are dehydrated at the same temperatures (100°C), the surface areas of the resultant oxides may be dependent on the number of OH^- attached to each metal cation in the hydroxide lattice. The formation of one Fe_3O_4 molecule involves the expulsion of 9 OH^- from the hydroxide lattice, whilst only 6 OH^- are expelled for the formation of Co_3O_4 . Thus, the resultant Fe_3O_4 should be finer than Co_3O_4 .

3.3. X-ray diffraction data

Fig. 2 shows the variation in lattice parameter, a_0 with the value of x in $\text{Co}_x\text{Fe}_{3-x}\text{O}_4$, confirming that cobalt-iron oxides have indeed been formed and that as Co replaces Fe in the spinel lattice, the unit cell decreases in size [19].

3.4. Electrical conductivity and activation energy for conduction in cobalt-iron oxides

Fig. 3 shows the variation of the logarithm of specific conductivity, σ with x . Since it is difficult to draw any definite conclusions on the variation of specific conductivity of compressed powders of different particle size [20], the specific conductivity of the samples was measured as a function of temperature as well. As seen from Fig. 4, the results for $\text{Co}_1\text{Fe}_2\text{O}_4$ indicate that a plot of $\log_{10}\sigma$ versus $1000/T$ yields a straight line with a positive slope, confirming that the sample exhibits semiconducting characteristics and that it is possible to obtain the activation energy for conduction with sufficient accuracy. Fig. 5 gives the variation of activation energy of conduction with x . The activation energy results provide a very much better indication of changes in con-

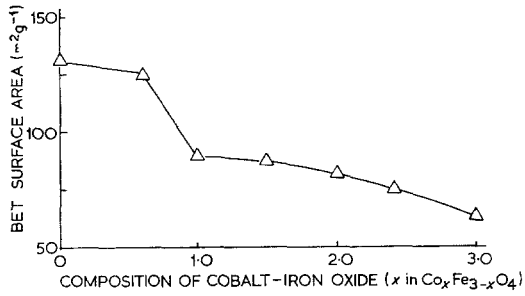


Figure 1 BET surface area as a function of cobalt-iron oxide composition (hydroxide preparation).

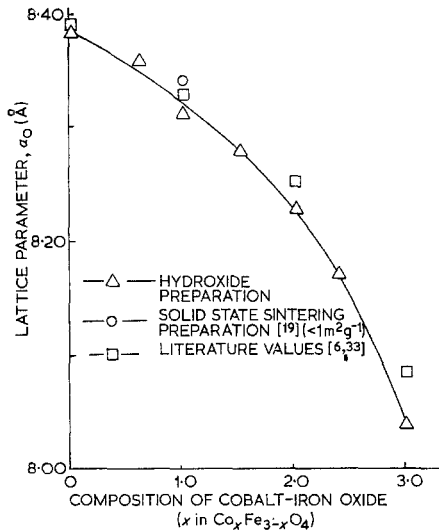


Figure 2 Variation of lattice parameter with cobalt-iron oxide composition.

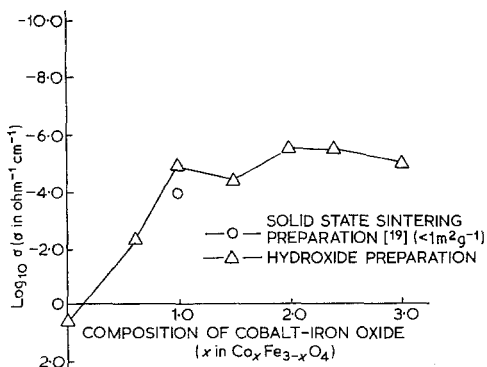


Figure 3 Specific conductivity (powder measurements at 25°C and 75% theoretical density) as a function of composition for cobalt-iron oxides.

ductivity since they are less dependent on particle size. Furthermore, the activation energies are largely unaffected by the frequency used

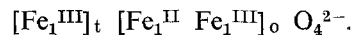
TABLE I Intended and actual composition of cobalt-iron oxides

Intended composition	Actual composition
$\text{Co}_0\text{Fe}_3\text{O}_4$	91% $\text{Co}_0\text{Fe}_3\text{O}_4$ + 9% Fe_2O_3
$\text{Co}_{0.6}\text{Fe}_{2.4}\text{O}_4$	94% $\text{Co}_{0.64}\text{Fe}_{2.36}\text{O}_4$ + 6% Fe_2O_3
$\text{Co}_{1.0}\text{Fe}_{2.0}\text{O}_4$	~99% $\text{Co}_{1.0}\text{Fe}_{2.0}\text{O}_4$
$\text{Co}_{1.5}\text{Fe}_{1.5}\text{O}_4$	~99% $\text{Co}_{1.5}\text{Fe}_{1.5}\text{O}_4$
$\text{Co}_{2.0}\text{Fe}_{1.0}\text{O}_4$	95% $\text{Co}_{1.9}\text{Fe}_{1.1}\text{O}_4$ + 5% Co_3O_4
$\text{Co}_{2.4}\text{Fe}_{0.6}\text{O}_4$	90% $\text{Co}_{2.3}\text{Fe}_{0.7}\text{O}_4$ + 10% Co_3O_4
$\text{Co}_{3.0}\text{Fe}_0\text{O}_4$	~99% $\text{Co}_{3.0}\text{Fe}_0\text{O}_4$

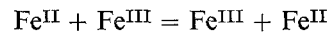
for the conductivity measurements [21]. Fe_3O_4 has the lowest activation energy for conduction (0.10 eV). This is comparable with the value of 0.05 eV reported by other workers [21]. Our samples have 5 to 10% $\alpha\text{-Fe}_2\text{O}_3$, which has a low conductivity (10^{-9} ohm $^{-1}$ cm $^{-1}$) [22]. This could account for the higher eV value. There is a peak in activation energy at the composition $\text{Co}_1\text{Fe}_2\text{O}_4$ (0.33 eV), after which the activation energy falls to $\text{Co}_{1.5}\text{Fe}_{1.5}\text{O}_4$ before increasing gradually again. A similar peak was found by Jonker [7] at compositions near $\text{Co}_1\text{Fe}_2\text{O}_4$ (0.42 eV).

3.5. Electronic structure of cobalt-iron oxides

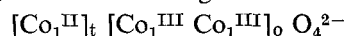
As indicated earlier, only the electronic structures of $\text{Co}_0\text{Fe}_3\text{O}_4$, $\text{Co}_1\text{Fe}_2\text{O}_4$, $\text{Co}_2\text{Fe}_1\text{O}_4$ and $\text{Co}_3\text{Fe}_0\text{O}_4$ have been described in the literature. $\text{Co}_0\text{Fe}_3\text{O}_4$ is an inverse spinel and accordingly possesses both ferrous and ferric ions on the octahedral sites;



Conduction can occur on the octahedral sites by hopping of charge carriers from one ion to the adjacent ion:



Equally important to the occurrence of semi-conductivity is the presence of suitable equivalent crystallographic sites. In the spinels, the octahedral site network furnishes the optimum framework for electron hopping, as with magnetite. There are both tetrahedral and octahedral sub-lattices available in the spinel structure, but no octahedral-tetrahedral interaction is possible. Thus $\text{Co}_3\text{Fe}_0\text{O}_4$, a normal spinel, has the following structure:



All the ions in the octahedral sites are Co^{III} , thus precluding any hopping mechanism. Furthermore, it is not possible for any interaction with the Co^{II} on the tetrahedral sites. This accounts for the low conductivity of Co_3O_4 .

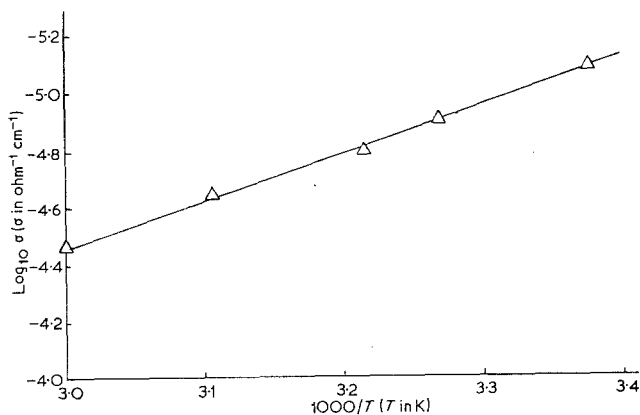


Figure 4 Specific conductivity for $\text{Co}_1\text{Fe}_2\text{O}_4$ (hydroxide preparation, powder measurements at 75% theoretical density) as a function of temperature.

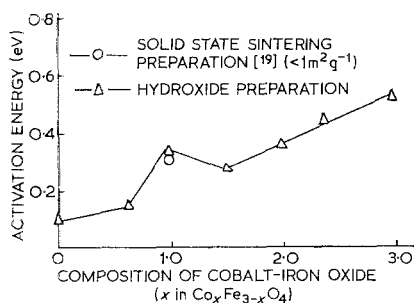


Figure 5 Activation energy for electrical conduction (powder measurements at 75% theoretical density) as a function of composition for cobalt-iron oxides.

Before the electronic structures of other cobalt iron oxides can be worked out, it is necessary to review the fundamental factors governing the site preference of cations in the spinel lattice. McClure [23], and Dunitz and Orgel [24] applied crystal field theory in conjunction with spectroscopic data to give quantitatively the d-shell splitting and the resulting stabilization of a

transition metal ion in a crystal site of given symmetry. The thermodynamic stabilization energy values may be found for both octahedral and tetrahedral sites in the AB_2O_4 spinel lattice and the difference between these values is the site preference energy (Table II).

Other second order effects [25] are likely to become significant when there is no appreciable site preference energy. On simple radius ratio grounds, larger cations prefer octahedral coordination, and smaller cations would preferentially occupy the tetrahedral sites. Since the trivalent cations in spinels are frequently smaller than the divalent ones, there is a tendency for them to occupy the tetrahedral sites, giving inverse distributions. However, coulombic attractions based on Madelung Energies for the configurations, tend to act in the opposite direction. Thus, the normal distribution is more stable than the inverse form in many spinels.

On the basis of the foregoing theoretical considerations, it is possible to assign electronic structures to all of the cobalt-iron oxides in-

TABLE II Properties of iron and cobalt ions*

Ion	Ionic radius Å	Number of d electrons	Stabilization energy (k cal mol ⁻¹)		Octahedral site preference energy (k cal mol ⁻¹)
			Octahedral site	Tetrahedral site	
Fe ^{II}	0.83	6	11.4	7.5	3.9
Fe ^{III}	0.67	5	0	0	0
Co ^{II}	0.82	7	17.1	15.0	2.1
Co ^{III}	0.63	6	45	26	19

*Compiled from [1, 23 and 24].

TABLE III Electronic structure of cobalt-iron oxides

Composition	Electronic structure	References
A $\text{Co}_0\text{Fe}_{3.0}\text{O}_4$	$[\text{Fe}_1^{\text{III}}]_t [\text{Fe}_{1.5}^{\text{II}}\text{Fe}_{1.5}^{\text{III}}]_o \text{O}_4^{2-}$ Inverse	[26, 27]
B $\text{Co}_{0.6}\text{Fe}_{2.4}\text{O}_4$	$[\text{Fe}_1^{\text{III}}]_t [\text{Co}_{0.6}^{\text{II}}\text{Fe}_{0.4}^{\text{II}}\text{Fe}_1^{\text{III}}]_o \text{O}_4^{2-}$	
C $\text{Co}_{1.0}\text{Fe}_{2.0}\text{O}_4$	$[\text{Fe}_1^{\text{III}}]_t [\text{Co}_1^{\text{II}}\text{Fe}_1^{\text{III}}]_o \text{O}_4^{2-}$ Inverse	[28-30]
D $\text{Co}_{1.5}\text{Fe}_{1.5}\text{O}_4$	$[\text{Co}_{0.5}^{\text{II}}\text{Fe}_{0.5}^{\text{III}}]_t [\text{Co}_{0.5}^{\text{II}}\text{Co}_{0.5}^{\text{III}}\text{Fe}_{1.0}^{\text{III}}]_o \text{O}_4^{2-}$	
E $\text{Co}_{2.0}\text{Fe}_{1.0}\text{O}_4$	$[\text{Co}_1^{\text{II}}]_t [\text{Co}_1^{\text{III}}\text{Fe}_1^{\text{III}}]_o \text{O}_4^{2-}$ Normal	[31]
F $\text{Co}_{2.4}\text{Fe}_{0.6}\text{O}_4$	$[\text{Co}_1^{\text{II}}]_t [\text{Co}_{1.4}^{\text{III}}\text{Fe}_{0.6}^{\text{III}}]_o \text{O}_4^{2-}$	
G $\text{Co}_{3.0}\text{Fe}_0\text{O}_4$	$[\text{Co}_1^{\text{II}}]_t [\text{Co}_2^{\text{III}}]_o \text{O}_4^{2-}$ Normal	[5]

vestigated in this paper (Table III). The structures of Fe_3O_4 , $\text{Co}_1\text{Fe}_2\text{O}_4$, $\text{Co}_2\text{Fe}_1\text{O}_4$ and Co_3O_4 have been firmly established by neutron diffraction and Mössbauer spectroscopy. Fe_3O_4 is fully inverse and in fact Fe^{II} does have a small octahedral site preference over Fe^{III} (Table II). Conversely, Co_3O_4 is normal. This is in accordance with d-shell splitting predictions in view of the large octahedral site preference of Co^{III} . Finally, $\text{Co}_1\text{Fe}_2\text{O}_4$ is reported as fully inverse, and this is to be expected from the small octahedral site preference of Co^{II} over Fe^{III} .

The electronic structure of $\text{Co}_{0.6}\text{Fe}_{2.4}\text{O}_4$ can be deduced from d-shell splitting considerations (Table II) and the known electronic structure of $\text{Co}_1\text{Fe}_2\text{O}_4$ - Fe^{II} enters the $\text{Co}_1\text{Fe}_2\text{O}_4$ lattice in place of Co^{II} to form $\text{Co}_{0.6}\text{Fe}_{2.4}\text{O}_4$ and prefers octahedral sites, giving rise to $[\text{Fe}_1^{\text{III}}]_t [\text{Co}_{0.6}^{\text{II}}\text{Fe}_{0.4}^{\text{II}}\text{Fe}_1^{\text{III}}]_o \text{O}_4^{2-}$. This is consistent with the fact that if all the Co^{II} were replaced, the fully inverse Fe_3O_4 structure would result.

The composition of $\text{Co}_{1.5}\text{Fe}_{1.5}\text{O}_4$ could similarly be written as $\text{Co}_1^{\text{II}}\text{Co}_{0.5}^{\text{III}}\text{Fe}_{1.5}^{\text{III}}\text{O}_4^{2-}$. Considering the change in composition from $\text{Co}_1\text{Fe}_2\text{O}_4$ to $\text{Co}_{1.5}\text{Fe}_{1.5}\text{O}_4$, there is a steady replacement of Fe^{III} by Co^{III} . The simplest way of satisfying d-shell predictions, is to introduce

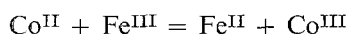
Co^{III} directly into the octahedral sites in place of Fe^{III} , giving $[\text{Fe}_1^{\text{III}}]_t [\text{Co}_1^{\text{II}}\text{Co}_{0.5}^{\text{III}}\text{Fe}_{0.5}^{\text{III}}]_o \text{O}_4^{2-}$ for $\text{Co}_{1.5}\text{Fe}_{1.5}\text{O}_4$. If this replacement continues, then $\text{Co}_2\text{Fe}_1\text{O}_4$ should have the inverse structure, $[\text{Fe}_1^{\text{III}}]_t [\text{Co}_1^{\text{II}}\text{Co}_1^{\text{III}}]_o \text{O}_4^{2-}$.

However, Blasse [6] on the basis of magnetic measurements, has postulated a normal distribution for $\text{Co}_2\text{Fe}_1\text{O}_4$. Thus, over the composition range $\text{Co}_1\text{Fe}_2\text{O}_4$ to $\text{Co}_2\text{Fe}_1\text{O}_4$, the spinel lattice changes from an inverse to normal distribution. It is possible, nevertheless, to suggest a mechanism for this without contravening d-shell splitting predictions. In comparing distributions C and E, the tetrahedral site occupancy must change from Fe^{III} to Co^{II} , although the net composition change from C to E is in Co^{III} replacing Fe^{III} . Accordingly, Co^{II} enters in place of Fe^{III} on the tetrahedral sites and simultaneously the corresponding amount of Co^{II} on the octahedral sites is shifted to the trivalent state as Co^{III} . The small loss in stabilization energy incurred when Co^{II} enters the lattice tetrahedrally, is easily compensated for from the large stabilization achieved when Co^{III} enters octahedrally. This results in distribution D for $\text{Co}_{1.5}\text{Fe}_{1.5}\text{O}_4$ and Blasse's distribution E for $\text{Co}_2\text{Fe}_1\text{O}_4$. Blasse did not

attempt to explain this inverse-normal change, and no explanation is apparent from simple theory. The octahedral site occupancy with high valency states of Co^{III} , Fe^{III} , evidently has greater stability than one with Co^{III} , Co^{II} .

The electronic structure of $\text{Co}_{2.4}\text{Fe}_{0.6}\text{O}_4$ can be derived by assuming that when excess Co^{III} replaces Fe^{III} in the octahedral sites in $\text{Co}_2\text{Fe}_1\text{O}_4$, it will give distribution F, whilst if the replacement is continued until the composition Co_3O_4 results, we will get the correct normal distribution (G).

The validity of the above electronic structures is confirmed by the results obtained for the activation energy for conduction versus composition (Fig. 5). For $x < 1$, the electron hopping between $\text{Fe}^{\text{II}}\text{Fe}^{\text{III}}$ on the octahedral sites is responsible for the conduction process. As seen from Table III, the number of $\text{Fe}^{\text{II}}\text{Fe}^{\text{III}}$ couples decrease as the value of x is increased. This accounts for the increase in activation energy for conduction between $0 < x < 1$. When $x = 1$, there is the possibility of $\text{Co}^{\text{II}}\text{Fe}^{\text{III}}$ exchange,



but hopping between ions of a different metal is likely to be more highly activated than for ions for the same metal, from orbital considerations. Nevertheless, this should result in a lower activation energy for $\text{Co}_1\text{Fe}_2\text{O}_4$ than for compounds such as Co_3O_4 , where no electron hopping is possible.

The higher activation energy required for conduction in $\text{Co}_2\text{Fe}_1\text{O}_4$ (0.34 eV) supports Blasse's formulation, E, for this compound and effectively rules out the alternative configuration with all the cobalt on the octahedral sites. This fixes the distribution of $\text{Co}_{1.5}\text{Fe}_{1.5}\text{O}_4$ and $\text{Co}_{2.4}\text{Fe}_{0.6}\text{O}_4$ as shown by D and F. The $\text{Co}^{\text{II}}/\text{Fe}^{\text{III}}$ distribution on tetrahedral sites for D is not expected to contribute much to the conductivity. The higher activation energies for $\text{Co}_{2.4}\text{Fe}_{0.6}\text{O}_4$ (0.43 eV) and Co_2O_4 (0.53 eV) show the increasing resistance of the system to passage of charge carriers as the lattice fills with Co^{III} on octahedral sites. Single crystal measurements on Co_3O_4 [32] give the conductivity at 20°C as $1.0 \times 10^{-4} \text{ ohm}^{-1} \text{ cm}^{-1}$ and the activation energy for conduction as 0.68 eV.

Thus, conductivity measurements have provided experimental results to augment theoretical predictions for the electronic structure of the

cobalt-iron oxide series.

Acknowledgement

This work was supported by the Science Research Council.

References

1. W. J. SCHUELE and V. D. DEETSCREEK, in "Ultrafine Particles", ed. W. E. Kuhn (John Wiley, New York, 1963) p. 224.
2. G. PARRAVANO, Fourth Int. Congress on Catalysis, Moscow 1968.
3. H. M. COTA, J. KATAN, M. CHIN, and F. J. SCHOENWEIS, *Nature* **203** (1964) 1281.
4. A. F. WELLS, "Structural Inorganic Chemistry" (Oxford University Press, 1962) p. 487.
5. J. P. SUCHET, "Chemical Physics of Semiconductors" (Van Nostrand, Amsterdam, 1965) p. 77.
6. G. BLASSE, *Philips Res. Reports* **18** (1963) 383.
7. G. H. JONKER, *J. Phys. Chem. Solids* **9** (1965) 165.
8. W. J. SCHUELE and V. D. DEETSCREEK, *J. Appl. Phys.* **32S** (1961) 235.
9. A. C. C. TSEUNG, and H. L. BEVAN, *J. Mater. Sci.* **5** (1970) 604.
10. T. SATO, M. SUGIHARA, and M. SAITO, *Rev. Elec. Commun. Lab.* **11** (1963) 26.
11. R. S. YOUNG, "Analytical Chemistry of Cobalt" (Pergamon Press, Oxford, 1965) p. 359.
12. J. SMILTENS, *J. Amer. Chem. Soc.* **79** (1957) 4881.
13. T. M. OVCHINNIKOVA, *Doklady Acad. Nauk SSR* **100** (1955) 469.
14. J. BESSON, Ph.D. Thesis, University of Paris (1957).
15. N. V. SIDGWICK, "The Chemical Elements and Their Compounds" (Oxford University Press, 1951) p. 1352.
16. C. L. WILSON and D. W. WILSON, *Comprehensive Analytical Chemistry* (Elsevier, Amsterdam, 1960) p. 170.
17. Y. A. FIALKOV and N. V. AXELRUD, *Ukr. Khim. Zh.* **16** (1950) 283.
18. W. C. ELMORE, *Phys. Rev.* **54**, (1938) 309.
19. J. R. YATES, B.Sc. Industrial Chemistry Project Report, The City University, London 1968.
20. W. R. HARPER, "Electrical Properties of Powders" (Eyre and Spottiswoode, London, 1961) p. 117.
21. F. C. ROMEIJN, *Philips Res. Reports* **8** (1953) 304.
22. GMELIN, "Handbuch der Anorganischen Chemie" (Verlag Chemie, 1959) Vol. 59D, p. 369.
23. D. S. MCCLURE, *J. Phys. Chem. Solids* **3** (1957) 311.
24. J. D. DUNITZ and L. E. ORGEL, *ibid* **3** (1957) 318.
25. J. GREENWALD, R. PICKART, and F. GRANIS, *J. Chem. Phys.* **22** (1954) 1957.
26. E. VERWEY, *Philips Res. Reports* **5** (1950) 173.
27. R. BAUMINGER and S. G. COHEN, *Phys. Rev.* **122** (1961) 743.
28. E. PRINCE, *ibid* **102** (1956) 674.

29. I. DEZSI, *Acta Phys. Polon.* **24** (1963) 283.

30. W. MÜLLER and H. SCHMALZRIED, *Ber. Bunsengesell. Physik. Chem.* **68** (1964) 270.

31. F. K. LOTGERING, *Philips Res. Reports* **11** (1956) 337.

32. B. M. HOCHBERG and M. S. SOMINSKI, *Phys. Z. Sowjetunion* **13** (1938) 198.

Received 30 March and accepted 11 May 1972.